Fibers and Polymers 2016, Vol.17, No.1, 74-79
DOI 10.1007/s12221-016-5721-7

ISSN 1229-9197 (print version)
ISSN 1875-0052 (electronic version)

Modeling Melt Blowing Fiber with Different Polymer Constitutive Equations

Wanli Han[1]* and Xinhou Wang[2,3]

[1]*Materials and Textile Engineering College, Jiaxing University, Jiaxing 314001, China*
[2]*College of Textiles, Donghua University, Shanghai 201620, China*
[3]*Key Laboratory of Textile Science & Technology, Ministry of Education, Shanghai 201620, China*
(Received September 25, 2015; Revised December 22, 2015; Accepted December 27, 2015)

Abstract: The characteristics of molten polymer plays a major role in fiber formation in the melt blowing (MB) process. In this paper, the Maxwell model and two kinds of the standard linear solid (SLS) models in the bead-viscoelastic element model are proposed for melt blown fiber formation simulation. The fiber diameter, velocity and stress are studied with these different constitutive equations of polymer. The trajectory path of fiber whipping is obtained using numerical simulation and compares with the actual fiber motion which is captured with a high-speed camera. The results present that the Standard Linear Solid Model (SLS) is better than Maxwell model to predict the melt blown fiber's characteristics under the same air drawing conditions, including fiber diameter, velocity and stress. The whipping motion of the fiber also can be well expressed by SLS constitutive model. The mathematical model with SLS model provides a clear understanding on the mechanism of the formation of microfibers during melt blowing.

Keywords: Melt blowing, The constitutive equations, Modeling, Fiber formation

Introduction

Nonwovens are commonly defined as a manufactured sheets or web of randomly or sometimes directionally oriented fibers, which are entangled or adhered by fibers without requiring any downstream processing such as weaving or knitting [1]. One of the most significant developments of this technology is melt blowing which involves applying a jet of hot air to an extruding polymer melt and drawing the polymer stream into microfiber with diameters. In general, the commercial melt blown nonwoven products are composed of fibers with average diameters exceeding 1-2 μm. Melt blowing is unique because it is used almost exclusively to produce microfibers rather than the size of normal textile fibers. Due to their extremely high surface to weight ratio, the microfiber nonwovens are useful in a variety of fields, such as biomedical, filter material, military and industrial applications [2,3].

Many significant efforts have been made to understand the technology and to improve the equipment by researchers and engineers around the world. Shambaugh and coworkers did a series of work on understanding the melt blowing process. Wu and Shambaugh [4] used laser Doppler velocimeter (LDV) to measure the cone diameters of fiber vibrations. Chhabra and Shambaugh [5] measured the fiber vibration with multiple-image flash photography. Bansal and Shambaugh [6] measured the fiber diameter and temperature during the melt blowing process via high speed flash photography and infrared camera. They [7-10] also used numerical simulation to analyze the velocity and temperature field and effects of the polymer fiber in the flow field from melt blowing die.

As to the air drawing model of a polymer in the melt blowing process, Uyttendaele and Shambaugh [11], Rao and Shambaugh [12], and Marla and Shambaugh [13] developed 1-dimensional, 2-dimensional, and 3-dimensional models to predict the fiber diameter, velocity and stress properties for melt blown fiber, respectively. The 2-dimensional and 3-dimensional models have taken special account into the fiber vibrations. The models incorporated a Newtonian or a viscoelastic Phan-Thien and Tanner constitutive equation, and they concluded over the range of parameters studied that there was very little effect of viscoelasticity on fiber diameter. These models indicated that viscoelasticity had very little impact on fiber diameter and attributed this to the rapid changes in temperature that occured during melt blowing process. Tan *et al.* [14] studied an initial and simplified model of melt blowing which included the influence of viscoelasticity and focused on how viscoelasticity affected the average fiber diameter at different air flow field. They have found that the variation in the meltblown fiber diameter depended on polymer viscoelasticity. However, their model assumed isothermal behavior and neglected energy equation. In fact, the thermal effects are important in practice. Besides, Ziabicki and Lewandowski [15,16] combined a 1-dimensional model of fiber dynamics with 3-dimensional turbulent air jet dynamics. The 1-dimensional model was based on the work of Uyttendaele and Shambaugh [11] but incorporated shear-induced crystallization and viscoelasticity. However, Ziabicki and Lewandowski only modeled several specific cases. They changed the molecular weight of the polymer in their model but did not provide insight into, for example, the role of viscosity vs. elasticity.

In our research group, we have been involved with extensive studies of various aspects of melt blowing process, including the coat-hanger die distribution [17,18], airflow field [19] and fiber model [20]. We developed a bead-

*Corresponding author: jxwlhan@163.com

viscoelastic element fiber model, and then adopted mixed Euler-Lagrange approach to simulate the three-dimensional fiber motion, especially the whipping motion in the process of melt blowing. In this paper, we turned our attention to the constitutive equation of fiber and described the influence of the constitutive equation of fiber in the melt blowing process. The Maxwell model and the standard linear solid model (SLS) were set as the constitutive equation of fiber respectively, and compared the variation of the fibers diameter, velocity and stress with these different constitutive equations. The trajectory path of fiber whipping was also simulated and compared with the actual fiber motion which was obtained with a high-speed camera.

Mathematical Description of a Fiber

The polymeric jet in the melt blowing process behaves like a non-Newton fluid. The jet is modeled as a series of beads connected by viscoelastic elements. A pair of adjacent beads, i–1 and i, form the fiber element (i–1, i), and the length of the element $l_{i-1,i}$ is given by

$$l_{i-1,i} = [(x_i - x_{i-1})^2 + (y_i - y_{i-1})^2 + (z_i - z_{i-1})^2] \quad (1)$$

The total number of beads, N, increases over time as new beads are inserted at the top of Figure 4 to represent the flow of melt polymer into the fiber.

Each bead is considered to represent the center of the mass of an element. The mass of bead i, m_i, is contributed by its adjacent fiber elements (i–1, i) and (i, i+1), thus, m_i is described as

$$m_i = \frac{1}{2}\rho_f (A_{i-1,i} l_{i-1,i} + A_{i,i+1} l_{i,i+1}) \quad (2)$$

where ρ_f is the fiber (polymer) density, $A_{i-1,i}$ and $A_{i,i+1}$ are the fiber cross-sectional areas of fiber elements (i–1, i) and (i, i+1), respectively, and are described as

$$A_{i-1,i} = \frac{1}{4}\pi d_{i-1,i}^2 \quad (3)$$

$$A_{i-1,i} = \frac{1}{4}\pi d_{i,i+1}^2 \quad (4)$$

where $d_{i-1,i}$ and $d_{i,i+1}$ are the diameters of fiber elements (i–1, i) and (i, i+1), respectively. For the first bead, bead 1, m_1 is contributed by the element (1, 2).

In melt blowing process, a molten stream of polymer is extruded into a high-velocity stream of forwarding gas and the force of the gas rapidly attenuates the fiber. The forces acting on the bead are: (1) external force $\mathbf{F}_{ex}$ such as gravity, aerodynamic force; (2) internal force $\mathbf{F}_{in}$ such as viscoelastic force; and (3) bending restoring force $\mathbf{F}_b$ to restore the rectilinear shape of the bending part of the jet. The total number of beads, N, increases over time as new beads are inserted at the top to represent the flow of solution or melt into the jet. Therefore, the equation for fiber motion is:

$$m_i \frac{d^2 r_i}{dt^2} = \mathrm{F}_{ex,i} + \mathrm{F}_{in,i} + \mathrm{F}_{b,i} \quad (5)$$

where $\mathbf{r}_i = \mathbf{i}x_i + \mathbf{j}y_i + \mathbf{k}z_i$ is the position of the ith bead; $\mathbf{F}_{ex,i}$, $\mathbf{F}_{in,i}$, $\mathbf{F}_{b,i}$ are external force, internal force, bending restoring force acting on bead i, respectively; **i**, **j**, and **k** are unit vectors in the xyz coordinate system.

During the Melt blowing process, the fiber temperature varies greatly. Assuming heat transfer within the fiber is neglected, the energy equation requires:

$$m_i C_i \frac{dT_i}{dt} = -h\pi \frac{d_{i-1,i} + d_{i,i+1}}{2} \frac{l_{i-1,i} + l_{i,i+1}}{2} (T_i - T_{ai}) \quad (6)$$

where C_i is the polymer heat capacity, T_i is the temperature of bead i, T_{ai} is the air temperature at bead i, and h is the convective heat transfer coefficient.

The detailed procedure of the simulation has been presented in our previous paper [15]. The constitutive equation of fiber will be discussed as follows.

The Constitutive Equation of Polymer

Fiber is one class of particles, which different general particulates in two factors: flexible and high aspect ratio. And the fiber model can be classified in two classes [18]: rigid model and flexible model. These two classes make fibers deform significantly during their motion. Therefore, to model the dynamic behavior of fiber model in melt blowing process, the development of a fiber model seems critical.

In our previous study, Maxwell constitutive equation model has been described in the melt blown fiber. The Maxwell model can be represented by a purely viscous damper and a purely elastic spring connected in series, as shown in the Figure 1.

In this configuration, under an applied axial stress, the total stress, σ_{Total} and the total strain, ε_{Total} can be defined

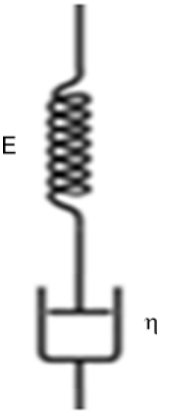

Figure 1. Maxwell model.

as follows:

$$\sigma_{Total} = \sigma_D = \sigma_S \tag{7}$$

$$\varepsilon_{Total} = \varepsilon_D + \varepsilon_S \tag{8}$$

where the subscript D indicates the stress/strain in the damper and the subscript S indicates the stress/strain in the spring. Taking the derivative of strain with respect to time, we can obtain:

$$\frac{d\varepsilon}{dt} = \frac{1}{E}\frac{d\sigma}{dt} + \frac{\sigma}{\eta} \tag{9}$$

$$\varepsilon(t) = \frac{\sigma_c}{E} + \frac{\sigma_c}{\eta}t \tag{10}$$

where E is the elastic modulus, σ_c is the constant stress and η is the material coefficient of viscosity.

This model is usually applied to the case of small deformations. From equation (10), it shows that the deformation is endless and can't recover when the stress is a constant number.

The standard linear solid (SLS) model is a method of modeling the behavior of a viscoelastic material using a linear combination of springs and dashpots to represent elastic and viscous components, respectively. It effectively combines the Maxwell Model and a Hookean spring in parallel. A viscous material is modeled as a spring and a dashpot in series with each other, both of which are in parallel with a lone spring. These elements are connected as shown in Figure 2.

For this model, the governing constitutive relation is:

$$\frac{(E_1 + E_2)\eta}{E_2}\frac{d\varepsilon}{dt} + E_1\varepsilon = \frac{\eta}{E_2}\frac{d\sigma}{dt} + \sigma \tag{11}$$

where E_1, E_2 is the elastic modulus and η is the material coefficient of viscosity.

The standard linear solid (SLS) model also has another configuration, the Kelvin-Voigt model and a Hookean spring are connected as shown In the Figure 3.

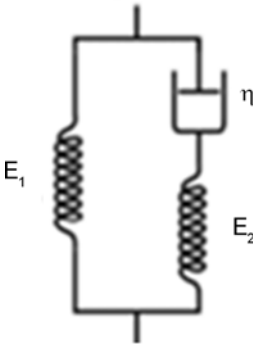

Figure 2. The standard linear solid (SLS) model (a).

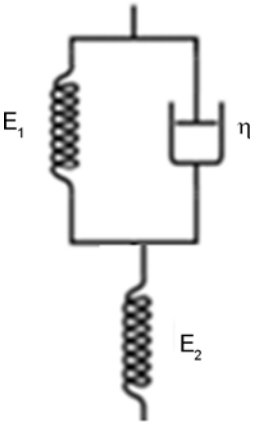

Figure 3. The standard linear solid (SLS) model (b).

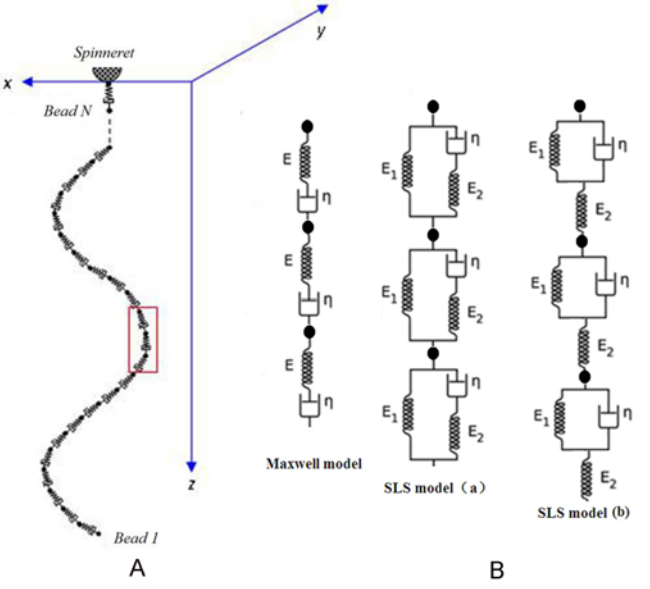

Figure 4. Schematic of a bead-viscoelastic element fiber model.

The governing constitutive relation can be described:

$$\frac{E_1\eta}{E_1 + E_2}\frac{d\varepsilon}{dt} + \frac{E_1E_2}{E_1 + E_2}\varepsilon = \frac{\eta}{E_1 + E_2}\frac{d\sigma}{dt} + \sigma \tag{12}$$

where E_1, E_2 is the elastic modulus and η is the material coefficient of viscosity.

The standard linear solid model combines aspects of the Maxwell and Kelvin-Voigt models to accurately describe the overall behavior of a system under a given set of loading conditions.

In this paper, the polymeric jet in the melt blowing process behaves as a viscoelastic non-Newton fluid. We model the jet as a series of beads connected by viscoelastic elements, as shown in Figure 4(A). The enlarged view of the part in the red window is shown in Figure 4(B), the fiber constitutive model are Maxwell model, the standard linear solid model (a) and the standard linear solid model (b) respectively. For

each constitutive equation of the fiber model simulation, the influence for fiber diameter, stress and velocity are studied and compared under the same airflow field.

The Air Flow Field of Melt Blowing

As the polymer exits the melt blowing die, the velocity of the air causes momentum transfer to the fiber, which results in rapid attenuation of the polymer. Unlike conventional melt spinning, the air jet used in melt blowing process not only provides a substantial forwarding force but also has a function of preventing polymer solidification. The air flow field of melt blowing plays an important role in fiber-formation process of melt blowing. In this study, a V-slot melt blowing die is used and the air flow field is obtained with numerical simulation. Figure 5(a) shows the computational domain which the slot height was fixed to be 5 mm. The computational domain below the die head was 100 mm× 30 mm (H=30 mm, W=100 mm). Three major geometry parameters of the slot die are slot width e, slot angle a, nose piece width f, which are 1.5 mm, 30° and 2 mm. In this simulation, the air was modeled as an ideal gas with Sutherland viscosity and k-ε turbulence model was used. As our previous research, the turbulence specifications of the inlet boundary were set with an intensity of 10 % and a hydraulic diameter equals to the slot width. While at the pressure outlets, turbulence intensity was 10 % and the length scale was 10 mm. the airflow field was obtained by solving the Navier-Stokes equations through the commercial software FLUENT 6.2. The contour of velocity of airflow field just below the die head, which is used in the fiber model, is shown in Figure 5.

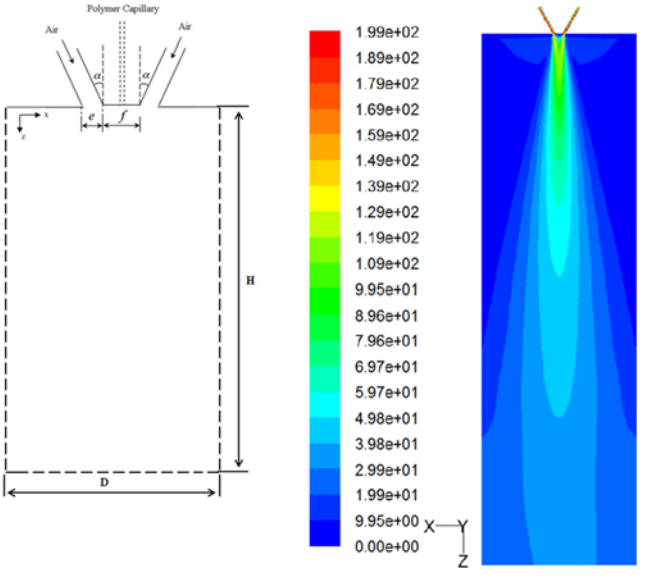

Figuer 5. Velocity contour of V-slot die (m/s).

Results and Discussion

In this paper, the fiber diameter, stress, and velocity were predicted and compared with different constitutive equations for fiber in these models under the same airfield condition.

Figure 6 indicates the effects on the fiber diameter with different constitutive equations of fiber. It illustrates that fiber diameter changes quickly for with SLS (b) model of fiber at the beginning. After z=0.1 m, all the models have the similar simulation result trends. SLS(a) model fiber gives the smallest fiber diameter which is closer to the experiment results [21,22]. This variation for fiber diameter attribute to fiber velocity as shown in Figure 7.

Figure 7 compares the fiber velocity and air velocity along the threadline for the different constitutive of fiber models. It shows that the air velocity quickly decreases as the distance from the die increasing. At the same time, the fiber velocity increases steadily and the rate of increase goes to zero at the

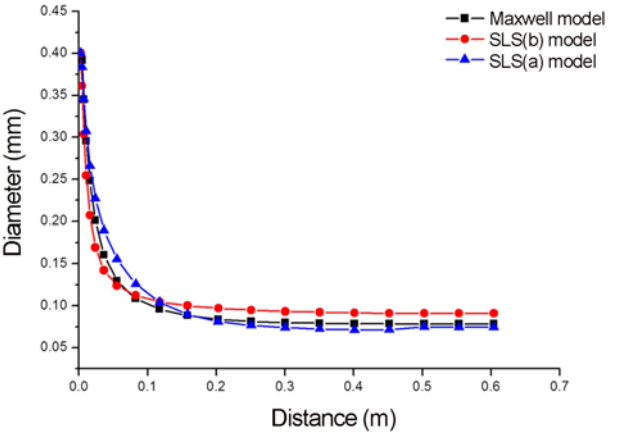

Figure 6. The fiber diameter for the different of constitutive of fiber model.

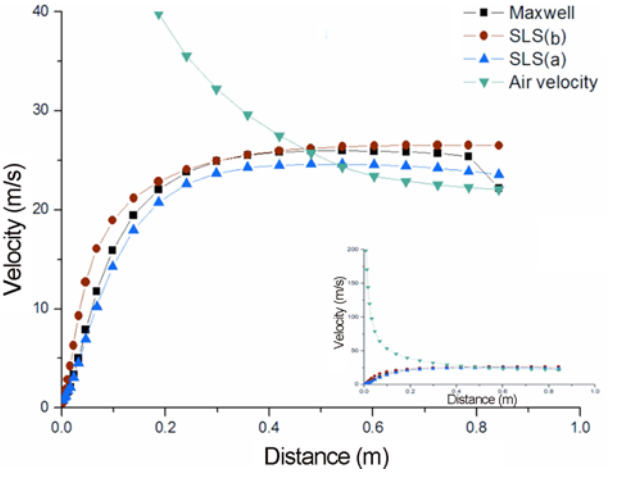

Figure 7. Comparison of the fiber velocity and air velocity along the threadline.

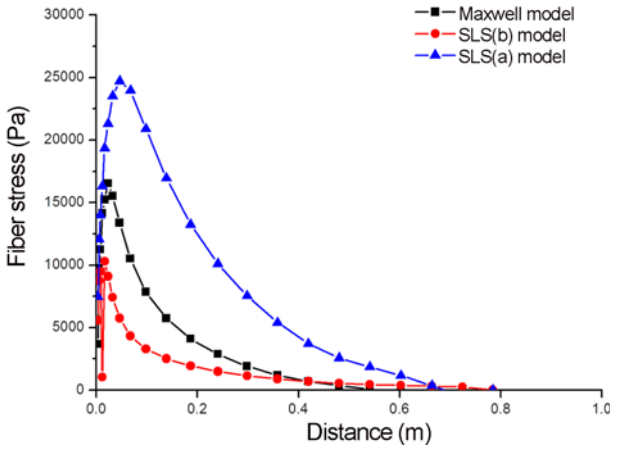

Figure 8. Effect of the constitute equation of fiber on the rheological stress.

stop point where the air velocity and fiber velocity are equal [14]. From Figure 7, it can be seen that the stop point of SLS(b) moves closer to the die than Maxwell model, and the SLS(a) moves the furthest to the die. That means the SLS(a) model fiber has more time to drawing in the airflow field and the diameter of fiber becomes smaller. Meanwhile, as the polymer jet exits the melt-blowing die, the velocity of the air causes momentum transfer to the fiber, which results in a rapid attenuation of the polymer. The relative velocity between fiber velocity and air velocity becomes higher under the slower velocity of fiber. This is the reason that the SLS(a) model fiber is the finest in Figure 6 and also has the largest of stress in the simulation in Figure 8.

Figure 8 illustrates the effect of the constitutive of fiber on the rheological stress of the fiber. The peak stress changes significantly with different constitutive equation. The largest of stress is simulated with SLS(a) model. As the different constitutive equations of fiber, the point of maximum stress also has different position for closing to the die. The predicted contours of fiber stress shows considerable accordance with the published experimental data of Bansal and Shambaugh [6].

Melt blowing process involves applying a jet of hot air to an extruding polymer melt and drawing the polymer stream into microfibers. According to Entov and Yarin's theory, when the air flow velocity incident on a jet exceeds a critical velocity, a small distance of the jet will grow and develop into bend instability and the fiber will take whipping motion. The fiber trajectory is an important dominant factor in drawing the fiber. Due to the jet curvature, the die to collector distance becomes longer and air drawing force will

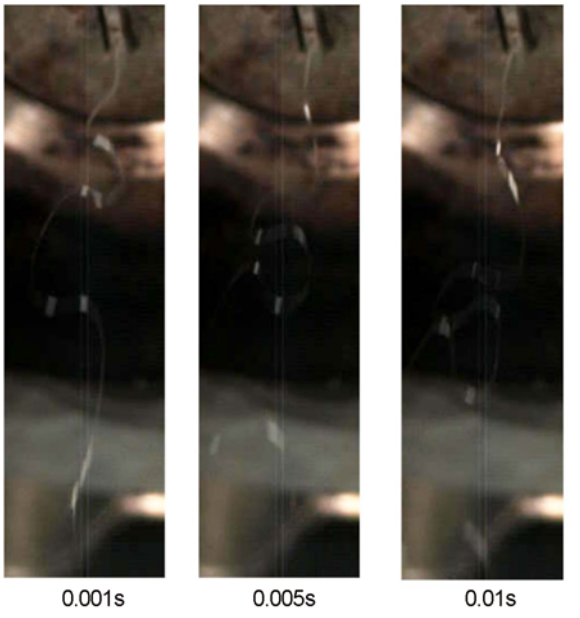

Figure 10. High-speed photographic image of motion for melt blowing fiber.

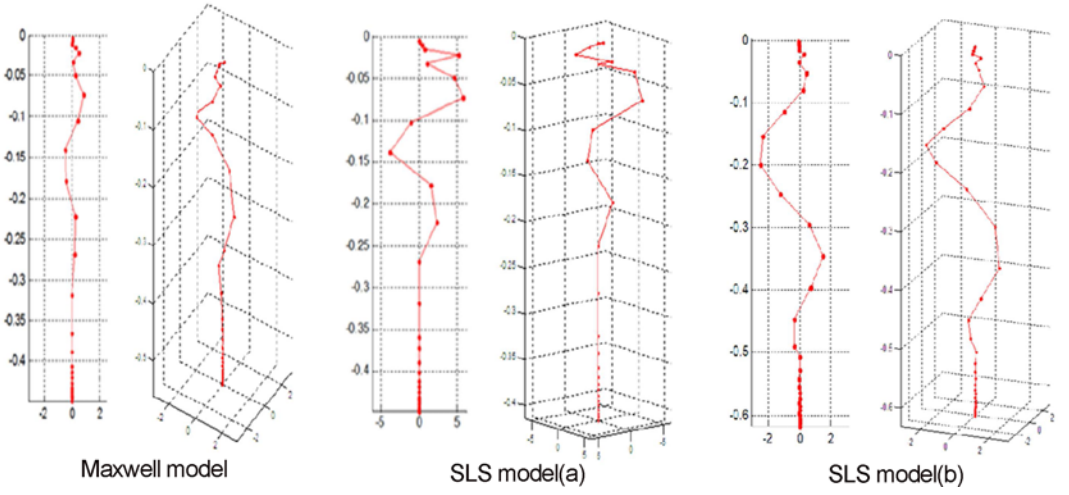

Figure 9. Melt blown fiber whipping motion at 0.05 s for three constitutive equations.

take more time to act on the polymer jet, which can make the perturbations grow and makes fiber diameter attenuation.

In this model, the fiber trajectory path is simulated using different constitutive equations, and the 0.005 s time evolution fiber path was shown in Figure 9. Meanwhile, three images of the fiber paths were taken by the Redlake camera during the operation of the single-orifice slot die melt-blowing process. A frame rate of 5000 frames/s was used with an exposure time of 0.2 ms. The image recording time was 0.001 s, 0.005 s and 0.01 s respectively in Figure 10.

Comparing with Figure 9 and Figure 10, it can be seen that the fiber path of simulation displayed a whipping motion generally similar with the image of experiment. Besides, the whipping amplitude of fiber motion path for SLS model is greater distance at the horizontal direction. The SLS model predicted bigger amplitude than the Maxwell model, which will result in the smaller fiber diameter due to the longer fiber path. The SLS model can predict the melt-blown fiber formation more accurately than the Maxwell model as the SLS model combines aspects of the Maxwell and Kelvin-Voigt models to accurately describe the overall behavior of a system under a given set of loading conditions. This result matches with our experimental phenomena in Figure 10.

Conclusion

In this paper, the Maxwell model and the Standard Linear Solid Model (a) and the Standard Linear Solid Model (b) constitutive equations were simulated to the melt blown fiber and the influence results of fiber diameter, velocity and stress were studied. The results presented that the Standard Linear Solid Model (SLS) could be used to predict the polymer's response very well under the same airflow field conditions. The fiber model with different constitutive equations also described the character of large aspect ratio, viscoelasticity and flexibility of the fiber and simulated the fiber formation in melt blowing process. The path of fiber in melt blowing is simulated and the SLS models fiber paths shows a perturbation development into the whipping and matches well with the experimental observation. The SLS model can provide an insight into the mechanism of the formation of microfibers during melt blowing.

Acknowledgments

This research was supported by National Natural Science Foundation of China (51506075), Jiaxing City bureau of Technology (2015AY11025).

References

1. S. J. Russell, "Handbook of Nonwovens", 1st ed., pp.1-5, CRC Press Inc., Boca Raton, FL. Cambridge, 2007.
2. R. R. Hegde and G. S. Bhat, *Appl. Polym. Sci.*, **115**, 1062 (2010).
3. Y. Zhang, C. Lim, S. Ramakrishna, and Z. M. Huang, *J. Mater. Sci.-Mater. Med.,* **16**, 933 (2005).
4. T. T. Wu and R. L. Shambaugh, *Ind. Eng. Chem. Res.,* **31**, 379 (1992).
5. R. Chhabra and R. L. Shambaugh, *Ind. Eng. Chem. Res*., **35**, 4366 (1996).
6. V. Bansal and R. L. Shambaugh, *Ind. Eng. Chem. Res*., **37**, 1799 (1998).
7. H. M. Krutka, R. L. Shambaugh, and D. V. Papavassiliou, *Ind. Eng. Chem. Res.*, **44**, 8922 (2005).
8. H. M. Kruka, R. L. Shambaugh, and D. V. Papavassiliou, *Ind. Eng. Chem. Res*., **45**, 5098 (2006).
9. H. M. Krutka, R. L. Shambaugh, and D. V. Papavassiliou, *Ind. Eng. Chem. Res.*, **46**, 655 (2007).
10. H. M. Krutka, R. L. Shambaugh, and D. V. Papavassiliou, *Ind. Eng. Chem. Res.*, **47**, 935 (2008).
11. M. A. J. Uyttendaele and R. L. Shambaugh, *AIChE J*., **36**, 175 (1990).
12. R. S. Rao and R. L. Shambaugh, *Ind. Eng. Chem. Res.,* **32**, 3100 (1993).
13. V. T. Marla and R. L. Shambaugh, *Ind. Eng. Chem. Res.,* **42**, 6993 (2003).
14. D. H. Tan, C. Zhou, C. J. Ellison, S. Kumar, C. W. Macosko, and F. S. Bates, *J. Non-Newton. Fluid Mech*., **165**, 892 (2010).
15. A. Zachara and Z. Lewandowski, *Fibres Text. East. Eur.,* **16**, 17 (2008).
16. L. Jarecki and Z. Lewandowski, *Fibres Text. East. Eur.*, **17**, 75 (2009).
17. W. L. Han and X. H. Wang, *Fiber. Polym*., **15**, 1190 (2014).
18. W. L. Han and X. H. Wang, *Fiber. Polym*., **13**, 626 (2012).
19. Y. F. Sun and X. H. Wang, *J. Appl. Polym. Sci*., **115**, 1540 (2010).
20. Y. F. Sun, Y. C. Zeng, and X. H. Wang, *Ind. Eng. Chem. Res.,* **50**, 1099 (2011).
21. S. Xie and Y. C. Zeng, *Fiber. Polym.*, **15**, 553 (2014).
22. S. Xie and Y. C. Zeng, *Ind. Eng. Chem. Res*., **52**, 2116 (2013).